Discrete Torsion of Connection Forms on Simplicial Meshes

THEO BRAUNE*, LIX, France
MARK GILLESPIE*, Inria, France
YIYING TONG, Michigan State University, USA
MATHIEU DESBRUN, Inria / LIX, France

While discrete (metric) connections have become a staple of n-vector field design and analysis on simplicial meshes, the notion of torsion of a discrete connection has remained unstudied. This is all the more surprising as torsion is a crucial component in the fundamental theorem of Riemannian geometry, which introduces the existence and uniqueness of the Levi-Civita connection induced by the metric. In this paper, we extend the existing geometry processing toolbox by providing torsion control over discrete connections. Our approach consists in first introducing a new discrete Levi-Civita connection for a metric with locally-constant curvature to replace the hinge connection of a triangle mesh whose curvature is concentrated at singularities; from this reference connection, we define the discrete torsion of a connection to be the discrete dual 1-form by which a connection deviates from our discrete Levi-Civita connection. We discuss how the curvature and torsion of a discrete connection can then be controlled and assigned in a manner consistent with the continuous case. We also illustrate our approach through theoretical analysis and practical examples arising in vector and frame design.

1 Introduction

Connections on manifolds play a key role in the modern theory of differential geometry. It is thus hardly surprising that discrete connections are used throughout geometry processing from the design of vector fields and stripe patterns on surfaces [Crane et al. 2010; Knöppel et al. 2015; Liu et al. 2016], to vectorization of 2D sketches [Guțan et al. 2023], and design tools for several forms of fabrication [Montes Maestre et al. 2023; Mitra et al. 2023, 2024]. In the smooth setting, connections on surfaces can be studied using Cartan's method of *moving frames*, where they are characterized by two quantities: their scalar-valued *curvature*, and their vector-valued *torsion*. However, existing work on connections focuses almost exclusively on curvature, neglecting torsion entirely.

---

*Both authors contributed equally to this research.

Authors' addresses: Theo Braune, LIX (IP Paris), Palaiseau, France, theo.braune@polytechnique.edu; Mark Gillespie, Inria Saclay (IP Paris), Palaiseau, France, mark.gillespie@inria.fr; Yiying Tong, Computer Science and Engineering, Michigan State University, East Lansing, USA, ytong@msu.edu; Mathieu Desbrun, Inria Saclay and Ecole Polytechnique (LIX, IP Paris), Palaiseau, France, mathieu.desbrun@inria.fr.

torsion potential

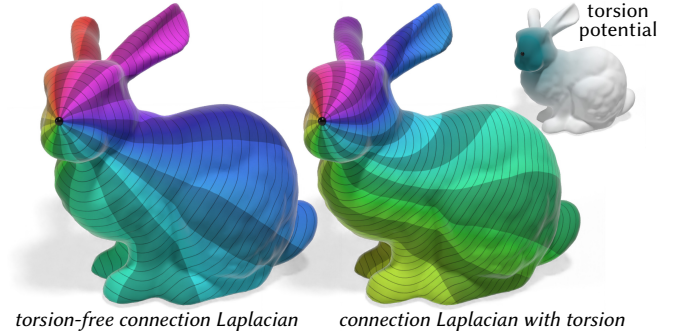*torsion-free connection Laplacian*   *connection Laplacian with torsion*

Fig. 1. **Torsion-controlled vector heat method.** The connection Laplacian used in the vector heat method of Sharp et al. [2019] can be formed for any connection. In this example, we compute a logarithmic map—a sort of global polar parameterization—using the connection Laplacian of an ordinary torsion-free connection *(left)*, and using a connection with prescribed non-zero torsion equal to the gradient of a torsion potential *(right)*, which introduces a distinct twist into the radial lines of the parameterization.

This paper enriches the geometry processing toolbox by introducing a discretization of torsion on triangle meshes and demonstrating its relevance to vector and frame field design applications.

2 Background and Related Work

Sections 2.1 and 2.2 review the relevant Riemannian geometry, and Sections 2.3 and 2.4 contrast our approach with existing work.

2.1 Vector Fields and Moving Frames

Vector field design is ubiquitous in geometry processing [de Goes et al. 2016; Vaxman et al. 2017]. The method of moving frames provides a convenient way of calculating with vector fields on smooth surfaces, and arises naturally in applications such as parameterization [Coiffier and Corman 2023], shape deformation [Corman 2024], and hexahedral meshing [Corman and Crane 2019; Fang et al. 2023].

Just as one can express a vector v in the plane as a linear combination of basis vectors e_1 and e_2, one can express a *vector field* $V(x)$ on a surface patch as a linear combination of *basis vector fields* $E_1(x)$ and $E_2(x)$, *i.e.*

$$V(x) = c^1(x)E_1(x) + c^2(x)E_2(x), \tag{1}$$

where $c^1(x)$ and $c^2(x)$ are scalar-valued coefficient functions. The basis fields E_1 and E_2 are often thought of as the columns of a single spatially-varying matrix $E(x)$, referred to as a *moving frame*. For simplicity, we will always assume that E is an *orthonormal*

frame. Note that it may be impossible to find a globally-defined moving frame—or even a single nonvanishing vector field (see the Poincaré–Hopf theorem). Hence, basis fields are usually defined locally: one can perform any desired calculation using different basis fields on each small patch, stitching the results together to obtain global results on the whole surface.

When working with moving frames, it is convenient to use the language of differential forms. Crane et al. [2013] provide a detailed introduction focused on the discrete theory, while Dray [2014] provides an introduction to the continuous theory. We make frequent use of the exterior derivative d, which generalizes curl and divergence to differential forms; the wedge product $\wedge$, which generalizes the cross product; the sharp operator $\sharp$, which uses the metric of a surface to map a differential 1-forms to corresponding vectors; and the Hodge star operator $\star_k$ which on surfaces turns k-dimensional differential forms into $(2 - k)$−dimensional forms.

2.2 Connections and Parallel Transport

While the directional derivative $D_X f$ of a scalar function f simply measures the rate of change of f as one moves along a tangential direction X, *directional derivatives of vector fields on surfaces* are more involved: vectors at different points on the surface belong to different tangent spaces, and *a priori* cannot be compared directly. A *connection* is a choice of operator $\nabla_X V$ acting as a directional derivative of a tangent vector field V in direction X; unlike the case of scalar functions, there are infinitely many meaningful connections.

Connections in a moving frame. If we pick a moving frame $E(x)$ to express our vector field $V(x)$ using its coefficient functions $c^1(x)$ and $c^2(x)$, then any connection can be written in the form
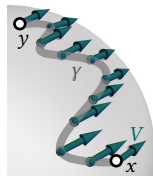
$$\nabla_X \begin{pmatrix} c^1(x) \\ c^2(x) \end{pmatrix} = \begin{pmatrix} D_X c^1(x) \\ D_X c^2(x) \end{pmatrix} + \begin{pmatrix} \omega_1^1(X) & \omega_2^1(X) \\ \omega_1^2(X) & \omega_2^2(X) \end{pmatrix} \begin{pmatrix} c^1(x) \\ c^2(x) \end{pmatrix}, \quad (2)$$

where the ω_i^j terms are *1-forms*, i.e., linear functions of a tangent vector X at point x. Different choices of 1-forms ω_i^j yield different connections. Equation 2 is often written more concisely as

$$\nabla = d + \omega, \quad (3)$$

where d is the componentwise exterior derivative, and ω is understood as a matrix-valued 1-form, known as the *connection 1-form*.

A connection allows us to *parallel transport* vectors along curves: if we have a vector V at point x, and a curve γ connecting x to another point y, we obtain a transported vector at y by taking the unique extension of V along γ whose directional derivative in the direction of γ stays identically zero.

The 1-form ω which we use to write our connection depends crucially on the choice of frame E: if we pick a new frame, we have to use a different connection 1-form to describe the exact same connection. These ω values are only meaningful locally, and do not fit together into a globally-defined matrix-valued 1-form on the whole surface. However, the *difference* between two connections is always a globally-defined 1-form. Indeed, connections form an *affine space*: starting from a connection ∇, we can write any other connection as the sum of ∇ and a globally-defined 1-form.

Metric-compatible connections. A connection ∇ is said to be *metric* if parallel transport preserves the lengths of vectors. Since our frame $E(x)$ is orthonormal, ∇ is a metric connection if and only if the connection 1-form ω is skew-symmetric, i.e., of the form

$$\omega(X) = \begin{pmatrix} 0 & -\alpha(X) \\ \alpha(X) & 0 \end{pmatrix}, \quad (4)$$

for some scalar-valued 1-form α. We restrict attention to metric connections, and often use the identification between matrix-valued connection 1-forms ω and the equivalent scalar-valued 1-forms α such that $\omega = \mathbb{J}\alpha$, where $\mathbb{J}$ denotes the matrix $\begin{pmatrix} 0 & -1 \\ 1 & 0 \end{pmatrix}$.

Curvature and torsion. As observed by Cartan, one can picture parallel transport as a description of the motion of a surface as it locally rolls around on the tangent plane of some point [Cartan 1923; Sharpe 1997]. Curvature and torsion capture two key features of this rolling behavior: curvature measures how much the surface rotates when rolled along an infinitesimal loop, while torsion measures how far it translates. Both curvature and torsion have simple expressions in the language of differential forms. If our connection is encoded by a connection 1-form ω in moving frame E, then the curvature of our connection is the matrix-valued 2-form $\Omega^\nabla = d\omega + \omega \wedge \omega$. For metric connections on surfaces, $\omega \wedge \omega = 0$, so the curvature is just

$$\Omega^\nabla = d\omega = \mathbb{J}d\alpha \quad (5)$$

For any pair of tangent vectors X, Y at some point p, the matrix $\Omega^\nabla(X, Y)$ describes the rotation applied to the tangent plane at p when the surface is rolled along the infinitesimal parallelogram spanned by X and Y. The component $d\alpha$ measures the rotation angle, and acts as a scalar measurement of curvature, generalizing the Gaussian curvature of a surface to arbitrary metric connections. The torsion of our connection is the vector-valued 2-form Θ^∇, with

$$\Theta^\nabla = d\theta + \omega \wedge \theta. \quad (6)$$

Here θ is the *dual frame* associated to our moving frame E, which takes in a tangent vector and returns the components of that tangent vector in the basis E. Unlike the connection 1-form ω, which is only defined relative to a choice of frame $E(x)$ in a local neighborhood, the curvature and torsion yield well-defined *global* 2-forms, meaningful in any coordinates on the surface.

Compatibility conditions between curvature and torsion. Starting from a given connection ∇ and for any globally-defined 1-form α, we can define a new connection as $\widetilde{\nabla} = \nabla + \mathbb{J}\alpha$. Note that

$$\mathbb{J}\alpha \wedge \theta = \alpha \wedge \mathbb{J}\begin{pmatrix} E^1 \\ E^2 \end{pmatrix} = \alpha \wedge \begin{pmatrix} -E^2 \\ E^1 \end{pmatrix} = -\begin{pmatrix} \alpha_1 \\ \alpha_2 \end{pmatrix} E^1 \wedge E^2, \quad (7)$$

where $\alpha = \alpha_1 E^1 + \alpha_2 E^2$ is expressed in the 1-forms (E^1, E^2) dual to E. Thus, the changes in curvature and torsion between the new and the old connections are given by

$$\Omega^{\widetilde{\nabla}} - \Omega^\nabla = \mathbb{J}d\alpha, \quad \text{and} \quad \Theta^{\widetilde{\nabla}} - \Theta^\nabla = -\alpha^\sharp \, dA, \quad (8)$$

which implies that these changes are linked: *the change in curvature is the curl of the change in torsion.*
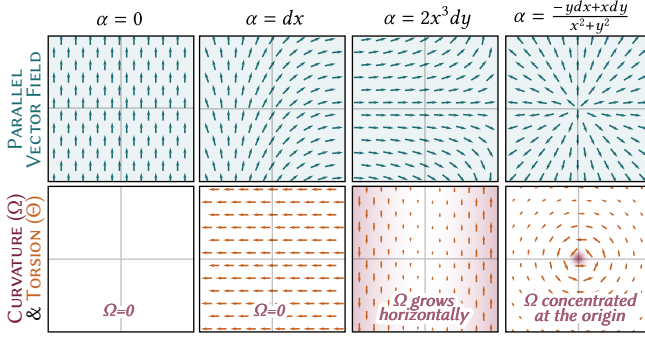
Fig. 2. **Metric-compatible connections.** Even in $\mathbb{R}^2$ equipped with the standard metric and standard basis, parallel transport of vectors by a metric connection may look very different from a simple translation. Here we consider four connection 1-forms α, and plot parallel vector fields for each connection *(top row)*, as well as the curvature *(bottom row, scalar density)* and torsion *(bottom row, vector field)* of each connection. All four connections are compatible with the standard metric—as their parallel fields are unit vector fields—but the rotations and singularities present in their parallel-transported vector fields can become arbitrarily complicated.

The Levi-Civita connection. For any metric on a surface, there is a unique metric connection with zero torsion. This connection, called the Levi-Civita connection $\nabla^{\text{LC}} = d + \mathbb{J}\alpha^{\text{LC}}$ encodes the geometry of the surface in important ways: for instance, the curvature of the Levi-Civita connection gives the surface's Gaussian curvature $\kappa = -d\alpha^{\text{LC}}$. And once you know the Levi-Civita connection, the calculation of curvature and torsion for all other connections also simplifies: Equation 8 shows that the curvature tensor of a connection $\widetilde{\nabla} = \nabla^{\text{LC}} + \mathbb{J}\alpha$ is $\mathbb{J}(d\alpha - \kappa dA)$, and the torsion $\Theta^{\widetilde{\nabla}}$ is

$$\Theta^{\widetilde{\nabla}} = -\alpha^\sharp \, dA. \tag{9}$$

This notion of torsion as a deviation from the Levi-Civita connection will be leveraged in our work.
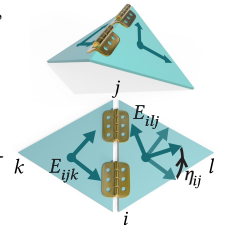
It is important to emphasize that the Levi-Civita connection is just one of many connections compatible with a given surface metric. While a metric connection preserves the lengths of vectors, it may not encode the surface geometry like the Levi-Civita connection does. For instance, the curvature of a metric connection may be completely different from the Gaussian curvature defined by the metric (Figure 2). The only relationship between them is that on closed surfaces, the connection curvature must obey the Gauss-Bonnet theorem: just like the ordinary Gaussian curvature, it must sum to 2π times the surface's Euler characteristic.

2.3 Connections on Discrete Surfaces

Most existing work using connections on triangle meshes follows the basic strategy of Crane et al. [2010] (or its dual variant), where one picks an arbitrary basis to encode tangent vectors in each face and then encodes the connection using an angle-valued dual 1-form giving the angle by which a vector must be rotated when parallel transporting it from one face to an adjacent one. These tangent bases on each face act as a globally-defined moving frame, allowing the connection to be represented as a discrete globally-defined 1-form,

without the need to use locally-defined frames on surface patches. The curvature of a discrete connection at a primal mesh vertex is then obtained by summing up the connection angles on the dual loop around that vertex. This curvature depends linearly on the connection 1-form, so is easy to find connections with any desired set of curvatures—such as trivial connections with only a few non-zero curvatures. However, while this strategy suffices to discretize curvature, no discrete notion of torsion was ever proposed.

A canonical connection on triangle meshes, that was leveraged by Crane et al. [2010] and which we will call the *hinge connection* η, is found by unfolding the hinge between two faces and measuring the angle η_{ij} between the chosen frames on these two faces (see inset, where the rotation angle η_{ij} aligns frame E_{ijk} with frame E_{ijl}). Crane et al. refer to this connection as "the discrete Levi-Civita connection", since its parallel transport is locally a translation in the isometric hinge map and its curvature is the usual discrete Gaussian curvature. Indeed, the hinge connection is exactly the Levi-Civita connection of the mesh, viewed as a polyhedral surface with piecewise-flat metric. Our approach also singles out this hinge map as a convenient "reference" connection from which we can encode other connections through dual 1-forms, but we also introduce a new discrete Levi-Civita connection which offers lower torsion (seen as the deviation from the Levi-Civita connection of an underlying smooth surface) by spreading vertex curvatures over dual faces. This spreading of curvature is reminiscent of the primal as-Levi-Civita-as-possible connection of Liu et al. [2016], which spreads curvature over primal faces, but Liu et al. use a more complex parameterization of vector fields, considering tangent vectors which may lie on mesh vertices, edges, or faces. Finally, we note that Braune et al. [2024] recently proposed a theory of discrete exterior calculus for vector-valued forms, leading to a definition of torsion for meshes via Equation 6. Unfortunately, their constructions are highly nonlinear, making it prohibitively difficult to solve for connections with prescribed torsions, or even for torsion-free connections.

2.4 Overview of Our Approach

In the remainder of this paper, we present a practical approach to torsion processing on surface meshes. First, we introduce a new discrete Levi-Civita connection which views a mesh not as a polyhedral surface with curvature concentrated at singularities, but as an approximation to a smooth surface with locally-constant curvature. We then describe how the discrete notion of torsion of a connection can be defined to mirror the continuous definition from Equation 9, i.e., we consider the discrete torsion of a connection as *the* discrete dual 1-form *by which a connection deviates from the discrete Levi-Civita connection*. This choice makes little difference in the continuous world, where the spaces of vector-valued 2-forms, vector fields, and 1-forms are all isomorphic. However, in our discrete setting, this discretization offers a practical and robust computational framework for torsion manipulation: we can trivially control the torsion of a connection while keeping its curvatures, and vice versa as shown on several geometry processing applications in Section 4.

3 Torsion on Discrete Surfaces

In this section, we first outline our notation in Section 3.1, and introduce a new discrete Levi-Civita connection which distributes curvature smoothly over dual faces in Section 3.2. From this low-torsion "reference" connection, we introduce a discrete notion of torsion modeled after Equation 9, *i.e.*, we define the torsion of a connection as the discrete dual 1-form by which it deviates from the discrete Levi-Civita connection. In Section 3.3, we review the various ways to prescribe torsion, with or without preserving curvatures.
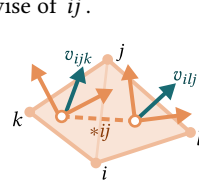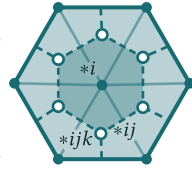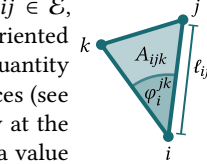
3.1 Notation and Conventions

Surface mesh and quantities. We work on a manifold triangle mesh $M = (\mathcal{V}, \mathcal{E}, \mathcal{F})$ with vertices $i \in \mathcal{V}$, edges $ij \in \mathcal{E}$, and faces $ijk \in \mathcal{F}$. We use $\vec{ij}$ to denote an oriented halfedge from i to j. A value u_i denotes a quantity u at vertex i, and similarly for edges and faces (see inset), while a value u_i^{jk} denotes a quantity at the corner of face ijk incident on vertex i, and a value $u_{\vec{ij}}$ denotes a quantity at halfedge $\vec{ij}$. For instance, the position of vertex i is $p_i \in \mathbb{R}^3$, the length of edge ij is $\ell_{ij} \in \mathbb{R}$, the area of face ijk is $A_{ijk} \in R$, and the angle at corner i of face ijk is $\varphi_i^{jk} \in [0, \pi)$. We use standard discrete exterior calculus operators such as the exterior derivatives $d_0 \in \mathbb{R}^{\mathcal{E} \times \mathcal{V}}$ and $d_1 \in \mathbb{R}^{\mathcal{F} \times \mathcal{E}}$ and Hodge star $\star_1 \in \mathbb{R}^{\mathcal{E} \times \mathcal{E}}$—see Crane et al. [2013] for more details.

Frame fields. A discrete frame field consists of a choice of frame per face of our mesh. These frames can be written explicitly as matrices $E_{ijk} \in \mathbb{R}^{3 \times 2}$ associated to each face ijk, where the two columns of E_{ijk} are orthonormal vectors in $\mathbb{R}^3$ tangent to face ijk. One can also store frames intrinsically as 2×2 matrices, interpreting the columns as tangent vectors in a fixed basis on face ijk. As mentioned in Section 2.2, we use $\mathbb{J}$ to denote 90° rotation matrix $\begin{pmatrix} 0 & -1 \\ 1 & 0 \end{pmatrix}$.

Dual mesh and orientations. We also consider the dual of M, which has a face $*i$ corresponding to each vertex of M, and edge $*ij$ corresponding to each edge of M, and a vertex $*ijk$ corresponding to each face of M. Our algorithm works with any choice of dual (*e.g.* circumcentric or barycentric), but we find that circumcentric duals can perform poorly on low-quality meshes (Section 4.4). As on the primal mesh, we denote value u on dual edge $*ij$ as u_{*ij}, *etc.* We also use $\vec{*ij}$ to denote the oriented halfedge running along dual edge $*ij$, picking the orientation that places $\vec{*ij}$ counterclockwise of $\vec{ij}$.

Discrete connections. A discrete metric connection provides a rotation angle $\alpha_{\vec{*ij}}$ on each halfedge describing how the coordinates of a vector v_{ilj} written in the frame of the right-hand face should be transformed to obtain a parallel-transported vector v_{ijk} in the frame of the left-hand face (see inset). As in the smooth setting, the angles α depend on the choice of frames, but once we write any connection α^0 in these frames, every other connection can be expressed as the sum of α^0 with a discrete dual 1-form. We follow Crane et al. [2010] and write our connections as offsets from the hinge connection η, but one could equally well pick any other connection to start from.
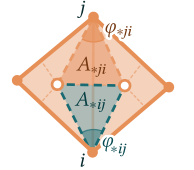
3.2 A New Discrete Levi-Civita Connection

As mentioned in Section 2.3, the hinge map is the exact Levi-Civita connection of a triangle mesh, viewed as a polyhedral surface with curvature concentrated at its vertices (see inset). However, this singular geometry differs in many ways from the geometry of the smooth surface which the mesh is supposed to approximate. We instead introduce a new connection $\omega^{\mathrm{LC}} = \mathbb{J}\alpha^{\mathrm{LC}}$ derived by spreading the curvature to be constant on each 1-ring instead. We find that this constant-curvature local approximation of the surface yields a connection with consistently lower error than the hinge map compared to the continuous Levi-Civita connection (Figure 5) without much added complexity. We propose a new connection written in closed form as an offset from the hinge map η_{ij} (Section 2.3) through the following expression:

$$\alpha_{ij}^{\mathrm{LC}} = \eta_{ij} + \frac{1}{\Diamond_{ij}} \left(K_i A_{*ij} \left(\frac{A_{*ij}}{A_i} - \frac{\varphi_{*ij}}{\Phi_i} \right) - K_j A_{*ji} \left(\frac{A_{*ji}}{A_j} - \frac{\varphi_{*ji}}{\Phi_j} \right) \right), \quad (10)$$

where A_{*ij} is the area of the triangle formed by dual edge $*ij$ and vertex i, φ_{*ij} is the corner angle of this triangle at vertex i, $\Diamond_{ij} = A_{*ij} + A_{*ji}$ is the area of the edge diamond, A_i is the area of the dual cell $*i$, Φ_i is the angle sum at vertex i, and K_i is the angle defect $2\pi - \Phi_i$, *i.e.* the integrated discrete Gaussian curvature. Note that in the case of a local region of the triangulation with only equilateral triangles, the ratios A_{*ij}/A_i and φ_{*ij}/Φ_i are all precisely $\frac{1}{6}$, and this connection reduces back to the hinge map. But in irregular regions, the two will generally differ. We provide the derivation of this expression in Appendix A, where we construct local constant-curvature connections in each vertex one-ring and stitch them together to define our discrete connection consistently over the whole mesh. The basic idea is that each vertex i has a total curvature K_i which must be distributed to its neighboring dual edges $*ij$. One can show that in our flattened one-ring parameterization, the hinge map distributes curvature proportional to the normalized tip angles φ_{*ij}/Φ_i, whereas our connection instead distributes curvature proportional to the incident areas A_{*ij}/A_i (and thus, the difference between the two connections in Equation 10 features both terms). The distinction is reminiscent of the calculation of vertex normals, where one may choose to average the incident face normals using area weights or angle weights.

3.3 Discrete Torsion of a Connection

Once we have a discrete Levi-Civita 1-form $\omega^{\mathrm{LC}} = \mathbb{J}\alpha^{\mathrm{LC}}$, we can understand torsion in the discrete realm via Equation 9: in the continuous case, the torsion of a connection measures its deviation from the Levi-Civita connection. We thus define the discrete torsion of a discrete connection $\omega = \mathbb{J}\alpha$ as the dual 1-form

$$\tau := \alpha - \alpha^{\mathrm{LC}}. \quad (11)$$

This definition exactly parallels the continuous definition and provides a simple and straightforward way not only to define torsion, but also to offer torsion processing on connections through Hodge decomposition [Crane et al. 2013] of this dual 1-form by controlling its curl, divergence, and harmonic components as we described next.
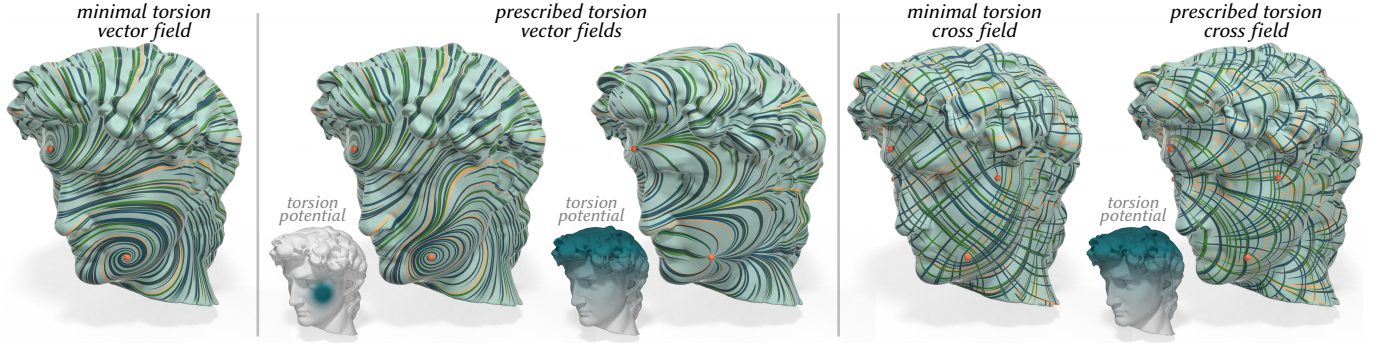
Fig. 3. **Torsion-controlled trivial connections.** Here we explore the impact of torsion on vector field design: a parallel vector field for a minimal-torsion trivial connection with prescribed singularities is shown on the left, while parallel fields for trivial connections with additional gradient components in their torsion are shown in the center, along with the prescribed scalar potentials. A compact potential changes the field locally *(center left)*, while a globally-supported potential causes larger-scale changes *(center right)*. Torsion can also be incorporated into the design of n-vector fields such as cross fields *(right)*.

Curl-constrained assignment of torsion. Since the curl of any change of torsion corresponds to a change in curvature (Equation 8), we can modify a connection $\omega = \mathbb{J}\alpha$ while keeping its curvature fixed by solving for a new connection whose torsion has the same curl. Explicitly, we maintain the connection's holonomy around collapsible dual cycles if and only if we add to α a harmonic dual 1-form, a dual gradient field $d_1^T f$ (where f is a dual 0-form, *i.e.*, a set of values on the mesh faces) — or both. Note that adding a harmonic form will affect the holonomy of each homology generator of the surface; so the higher the genus of a surface, the more ways the torsion can be edited, which can potentially be useful in applications such as quadrangulation, *e.g.*, with holonomy of multiples of $\pi/2$.

Divergence-constrained assignment of torsion. Conversely, given a discrete connection $\omega = \mathbb{J}\alpha$, one can preserve the divergence of its torsion by adding $\star_1 d_0 p$ for a scalar potential p defined on vertices. As the additional connection is the $90°$–rotated gradient of p, it is divergence-free, and will not alter the above-mentioned gradient component of torsion $d_1^T f$. In other words, such a perturbation is the minimal change needed to modify the connection's curvature.

We show examples of torsion editing in Section 4 to emphasize how torsion affects the notion of parallel transport in various geometry processing applications.

3.4 Trivial Connections

Crane et al. [2010] proposed to design tangent n-vector fields over a given mesh by prescribing their singularities and associated indices. They solve for a metric connection — dubbed a trivial connection — with zero holonomy around all mesh vertices and around the generators if the genus is non-trivial, except on each of the singularities where the holonomy is set based on the singularity index. These constraints amount to a set of linear equations fixing the curvature around each vertex and the holonomy about each homology generators. Since these linear constraints are less numerous than the number of dual edges, the authors proposed taking the solution with the minimal L^2 norm, reasoning that this choice ensures that the connection is as close to the original hinge connection, and thus perturbs the notion of parallel transport the least. The final vector field

with prescribed singularities is then constructed from an arbitrary unit vector on a face that is parallel-transported throughout the mesh via this new connection. Since the connection is compatible with the metric, this construction generates a unit vector field.

Our discrete theory of torsion introduces a new interpretation of this optimization problem: the L^2 norm that Crane et al. minimize is akin to our Equation 11, except that it measures the distance to the hinge map rather than the distance to our new discrete Levi-Civita connection. Moreover, we obtain a new geometric interpretation of the space of trivial connections with prescribed singularities—these are precisely the connections whose torsion 1-forms have a fixed curl. Inside this space, we can move beyond the idea of minimizing torsion to explore the effects of prescribing different torsions. As discussed in Section 3.3, we can easily ensure that our new torsion obeys the curl constraints as long as we only modify it by adding the gradient of a scalar potential. As Figure 3 demonstrates, this alteration of the trivial connection may have a substantial impact.

4 Evaluation and Results

Now we explore the effect of torsion prescription in scenarios like n-vector field design (Section 4.1), connection Laplacians (Section 4.2), before moving on to discuss convergence to ground-truth analytic connections in several scenarios (Section 4.3), and discussing the choice of dual mesh (Section 4.4).

4.1 N–Vector Field Design

As observed by Crane et al. [2010], one can use a connection to design tangent vector fields on a surface: if we have a connection, we can obtain a vector field by picking one vector at an arbitrary point, and parallel transporting that vector to all other points of the surface. The resulting vector field will be continuous if and only if the connection is *trivial*—meaning that its curvature at every vertex is a multiple of 2π, as its holonomy around every loop.

As discussed in Section 3.4, imposing these curvature constraints fixes the curl and harmonic components of the torsion, leaving exactly the torsion's gradient component free to prescribe. In Figure 3 we show several vector fields generated from different trivial connections all sharing the same curvature constraints. In general,

optimized via Levi-Civita connection Laplacian

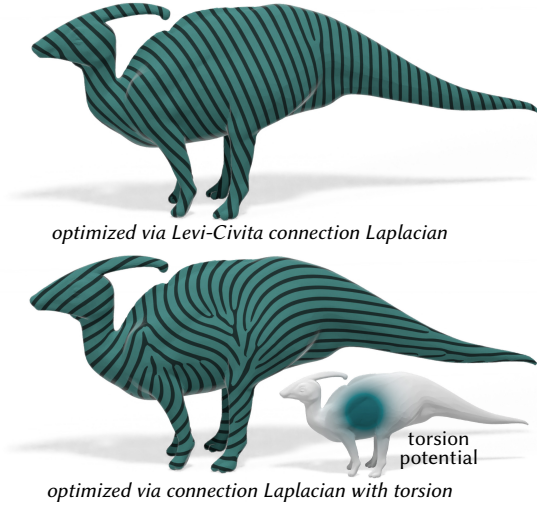*optimized via connection Laplacian with torsion*

Fig. 4. **Optimal vector fields for different connections.** Just as the ordinary Laplacian measures the smoothness of scalar functions, the connection Laplacian defines a notion of smoothness for vector fields. Computing an optimal vector field in the sense of Knöppel et al. [2013] using the discrete Levi-Civita connection to build the connection Laplacian yields a field whose streamlines are as straight as possible in 3D space *(top)*, whereas using a connection with a nontrivial torsion (here, the gradient of a potential) introduces twists into the streamlines *(bottom)*.

modifying the torsion by the differential $d_1^T f$ of a potential function f will introduce a twist into the parallel vector fields, with more twist in regions where the magnitude of f is greater.

The case of n-vector field design is no different: setting singularities with indices being multiple of $2\pi/n$ will generate tangent direction fields that are smooth up to local rotations by multiples of $2\pi/n$, such as cross fields for instance for $n=4$ (Figure 3, *right*).

4.2 Connection Laplacians

A connection on a surface can also be used to define a *connection Laplacian*, which measures the smoothness of vector fields just as the ordinary Laplacian measures the smoothness of scalar functions. This connection Laplacian thus plays an important role in algorithms throughout geometry processing [Knöppel et al. 2013; Liu et al. 2016; Sharp et al. 2019], and our connections can be directly used to construct more general dual connection Laplacians for face-based vector fields. In the primal setting, it is also easy to add a primal 1-form to any choice of connection to obtain a primal connection Laplacian with torsion. Figure 1 illustrates the impact of torsion on the vector heat method of Sharp et al. [2019], where the (primal) connection Laplacian is used to solve a discrete vector diffusion problem, approximating parallel transport of vectors along shortest paths. As pointed out by Sharp et al. [2019, §6.1.3] using a connection Laplacian for a new connection then approximates parallel transport using your new connection. Sharp et al. show that one can apply vector diffusion to a pair of vector fields to compute a *logarithmic map*, approximating the distance and direction from a single source vertex to all other vertices. By modifying one of
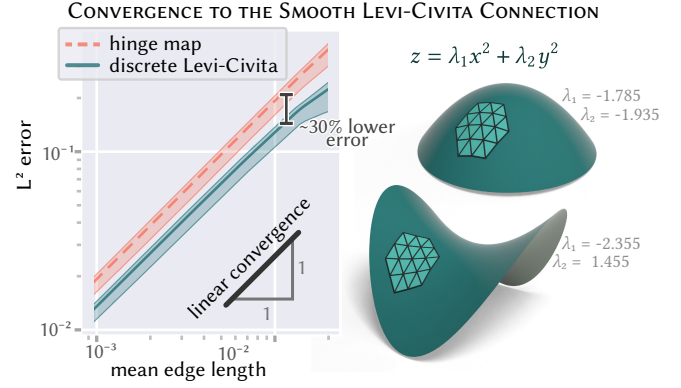
Fig. 5. **Convergence test.** Here we plot the L^2 errors of the hinge map vs. our discrete Levi-Civita connection compared to the smooth Levi-Civita connection on several hundred randomly generated quadratic surfaces. The plotted lines show the average error across all experiments, while shaded envelopes show the maximum and minimum errors. Both discrete connections converge at the same linear rate, but our discrete Levi-Civita connection offers lower error in every case. Two sample surfaces are shown on the right

the diffusion equations to use a connection with torsion, we can effectively "twist" the polar parameterization.

As another example, Knöppel et al. [2013] proposed an algorithm to compute smooth direction fields as eigenfunctions of a connection Laplacian. Using a connection Laplacian with torsion encourages a similar twisting behavior in direction fields, creating interesting branching patterns if the direction fields are visualized using the stripe pattern algorithm of Knöppel et al. [2015], see Figure 4.

4.3 Convergence

In this section, we measure the convergence of our discrete connections to analytic solutions under mesh refinement.

Convergence of our discrete Levi-Civita connection. In Figure 5, we plot the L^2 errors of the hinge map and our discrete Levi-Civita connection compared to the true Levi-Civita connection on smooth surfaces of the form $z = \lambda_1 x^2 + \lambda_2 y^2$. These examples are universal, in the sense that locally, any smooth surface can be approximated up to second order by a quadratic surface $z = ax^2 + bxy + cy^2$, and moreover any such quadratic form can be diagonalized by a simple rotation of the xy-plane, reducing to the simple quadratic surfaces which we consider. We generated 500 random quadratic surfaces with values of λ_1 and λ_2 chosen uniformly at random in the range of $[-2.5, 2.5]$. As expected, both discrete connections converge linearly under refinement, but our discrete Levi-Civita connection has consistently lower error than the hinge map — around 30% lower in this particular example. To ensure that we compare the accuracy of the two connections over the whole surface, rather than merely along dual edges, we measure the error in each vertex one-ring by fitting a linear 1-form to the discrete connection values on the adjacent dual edges, and compute the L^2 distance to a 2nd-order-accurate approximation to the smooth Levi-Civita connection within this region—we provide a derivation of the reference solution in Section 2 of the supplemental material.

Convergence of trivial connections. Our identification of torsion with deviation from the Levi-Civita connection allows us to derive closed form expressions for trivial connections with prescribed singularities on smooth surfaces. In Appendix C we derive an analytic expression for minimal-torsion trivial connections on the sphere, and in Figure 6, we plot the L^∞ error of trivial connections on the sphere computed starting from our discrete Levi-Civita connection, and from the hinge map, compared to an analytic reference solution with minimal torsion and one with nonzero prescribed torsion. Because the ground truth trivial connection blows up near the singularities, we measure the error on a small surface patch away from the singularities. Note that the prescribed torsion arising from the potential is captured almost perfectly by the discretization, so both trivial connections have near-identical errors.
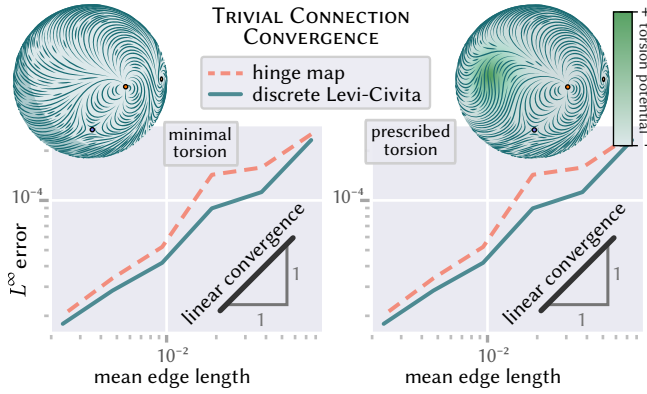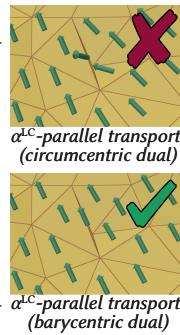

Fig. 6. **Convergence to trivial connections.** Here we plot the L^∞ error of a discrete trivial connections compared to an analytic reference solution with minimal torsion *(left)* and with prescribed torsion *(right)*. Since the solutions blow up around singularities, we measure the error on a patch of the sphere away from the singularities.
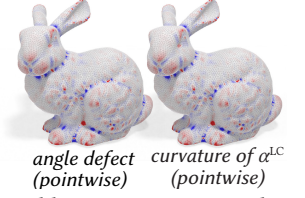
4.4 Sensitivity to Dual Mesh

We finally point out that the choice of dual mesh can have an impact on the robustness of our discrete Levi-Civita connection. The use of the circumcentric dual simplifies many expressions (*e.g.*, the half-diamond areas A_{*ij} and A_{*ji} in Equation 10 become equal, and the angle φ_{*ij} subtended by a dual edge can be written explicitly in terms of the corner angles opposite edge ij as $\pi - \varphi_k^{ij} - \varphi_m^{ji}$). However, using the circumcentric dual may lead to flipped dual edges (even on otherwise high-quality meshes), which may lead to large numerical errors. In practice, we find that implementing our method using the barycentric dual mesh leads to significantly less sensitivity to triangle quality without requiring a large increase in implementation complexity or degrading solution quality on well-conditioned meshes. Other choices, such as the hybrid approach of Meyer et al. [2003], may be adopted instead.

α^{LC}-*parallel transport (circumcentric dual)*

α^{LC}-*parallel transport (barycentric dual)*

5 Future Work

Our work opens up a number of questions and interesting research directions which we briefly mention next.

Curvature of α^{LC}. In general, the curvature of our discrete Levi-Civita connection α^{LC} is not exactly equal to the curvature of the hinge map, *i.e.*, the angle defect K_i. The curvature of α^{LC} at a vertex i is given by K_i plus some corrections terms in-

angle defect (pointwise)   *curvature of α^{LC} (pointwise)*

volving the angle defects K_j of the neighboring vertices. On the circumcentric dual, one can show that the curvature of α^{LC} at i is equal to $K_i + \frac{1}{2} \sum_{ij>i} K_j \left(A_{*ji}/A_j - \varphi_{*ji}/\Phi_j \right)$, meaning that the curvature at vertex i receives a small contribution from the angle defects of its neighbors, where the exact contribution depends on the local regularity of the triangulation. In practice, the two curvature estimates are usually quite similar (see inset), although they can differ significantly around sharp vertices and other mesh degeneracies. It would be interesting to investigate whether this curvature is related to other common estimates of Gaussian curvature, and to more precisely characterize the smoothing effects on other duals.

Alternative metrics. We focused on connections compatible with the metric of the input mesh, but sometimes one may want connections arising from other metrics. For instance, minimal-torsion trivial connections can be seen as Levi-Civita connections for cone metrics which concentrate all curvature at the singularities of the trivial connection. This change in perspective essentially adapts the metric to remove singularities in the connection, which could potentially lead to better-conditioned problems in cases with extreme singularities. While finding an explicit mesh with such a metric is nontrivial, the local geodesic polar maps which we use in our derivations in the appendix can be adapted to accommodate different metrics on the input surface using only curvature information (precisely the information provided in a trivial connections problem). The curvature in a vertex one-ring is simply used to rescale the polar coordinate basis vectors at the beginning of our calculations (see *e.g.* Equation 18), which can be done for any desired curvatures

Torsion of connections in higher dimension. Measuring the twisting of fields in $\mathbb{R}^3$ is a fundamental problem in mathematics and physics [Binysh and Alexander 2018] which arises in areas of graphics like volumetric meshing [Corman and Crane 2019] and fluid simulation [Ishida et al. 2022]. A discrete theory of torsion for three-dimensional connections could be a key tool for studying and optimizing such fields. But torsion on 3-manifolds is far more complicated than on surfaces: on surfaces torsion can be encoded by a vector field rather than a vector-valued 2-form (Equation 9), but in higher dimensions such a straightforward characterization is no longer possible. The closest analogue is the decomposition of Cartan [1925, Chapter 8], which breaks down the torsion tensor into a "vectorial" component, a 3-form component, and a third component. Unfortunately, "the third torsion component has no geometric interpretation" [Agricola and Kraus 2016], making it difficult to use as the basis for a discrete theory of torsion on volumes.

Acknowledgments

References

Ilka Agricola and Margarita Kraus. 2016. Manifolds with Vectorial Torsion. *Differential Geometry and its Applications* 45 (2016), 130–147. https://doi.org/10.1016/j.difgeo.2016.01.004

Jack Binysh and Gareth P. Alexander. 2018. Maxwell's theory of solid angle and the construction of knotted fields. *Journal of Physics A: Mathematical and Theoretical* 51, 38 (2018), 385202. https://doi.org/10.1088/1751-8121/aad8c6

Theo Braune, Yiying Tong, François Gay-Balmaz, and Mathieu Desbrun. 2024. A Discrete Exterior Calculus of Bundle-valued Forms. arXiv:2406.05383 [math.DG]

Elie Cartan. 1923. Sur les variétés à connexion affine et la théorie de la relativité généralisée (première partie). *Annales scientifiques de l'École Normale Supérieure* 40, 3 (1923), 325–412. https://doi.org/10.24033/asens.751

Elie Cartan. 1925. Sur les variétés à connexion affine, et la théorie de la relativité généralisée (deuxième partie). *Annales scientifiques de l'École Normale Supérieure* 42 (1925), 17–88. https://doi.org/10.24033/asens.761

Guillaume Coiffier and Etienne Corman. 2023. The Method of Moving Frames for Surface Global Parametrization. *ACM Transactions on Graphics* 42, 5, Article 166 (2023). https://doi.org/10.1145/3604282

Etienne Corman. 2024. Curvature-Driven Conformal Deformations. *ACM Transactions on Graphics* 43, 4, Article 139 (2024). https://doi.org/10.1145/3658145

Etienne Corman and Keenan Crane. 2019. Symmetric Moving Frames. *ACM Transactions on Graphics* 38, 4, Article 87 (2019). https://doi.org/10.1145/3306346.3323029

Keenan Crane, Fernando de Goes, Mathieu Desbrun, and Peter Schröder. 2013. Digital Geometry Processing with Discrete Exterior Calculus. In *ACM SIGGRAPH 2013 Courses*. https://doi.org/10.1145/2504435.2504442

Keenan Crane, Mathieu Desbrun, and Peter Schröder. 2010. Trivial Connections on Discrete Surfaces. *Computer Graphics Forum* 29, 5 (2010), 1525–1533. https://doi.org/10.1111/j.1467-8659.2010.01761.x

Fernando de Goes, Mathieu Desbrun, and Yiying Tong. 2016. Vector Field Processing on Triangle Meshes. In *ACM SIGGRAPH 2016 Courses*. Article 27. https://doi.org/10.1145/2897826.2927303

Tevian Dray. 2014. *Differential Forms and the Geometry of General Relativity*. CRC Press. https://doi.org/10.1201/b17620

Xianzhong Fang, Jin Huang, Yiying Tong, and Hujun Bao. 2023. Metric-Driven 3D Frame Field Generation. *IEEE Transactions on Visualization and Computer Graphics* 29, 4 (2023), 1964–1976. https://doi.org/10.1109/TVCG.2021.3136199

Olga Guțan, Shreya Hegde, Erick Jimenez Berumen, Mikhail Bessmeltsev, and Edward Chien. 2023. Singularity-Free Frame Fields for Line Drawing Vectorization. *Computer Graphics Forum* 42 (2023), e14901. https://doi.org/10.1111/cgf.14901

Sadashige Ishida, Chris Wojtan, and Albert Chern. 2022. Hidden Degrees of Freedom in Implicit Vortex Filaments. *ACM Transactions on Graphics* 41, 6, Article 241 (2022). https://doi.org/10.1145/3550454.3555459

Felix Knöppel, Keenan Crane, Ulrich Pinkall, and Peter Schröder. 2013. Globally Optimal Direction Fields. *ACM Transactions on Graphics* 32, 4, Article 59 (2013). https://doi.org/10.1145/2461912.2462005

Felix Knöppel, Keenan Crane, Ulrich Pinkall, and Peter Schröder. 2015. Stripe Patterns on Surfaces. *ACM Transactions on Graphics* 34, 4, Article 39 (2015). https://doi.org/10.1145/2767000

Beibei Liu, Yiying Tong, Fernando De Goes, and Mathieu Desbrun. 2016. Discrete Connection and Covariant Derivative for Vector Field Analysis and Design. *ACM Transactions on Graphics* 35, 3, Article 23 (2016). https://doi.org/10.1145/2870629

Mark Meyer, Mathieu Desbrun, Peter Schröder, and Alan H. Barr. 2003. Discrete Differential-Geometry Operators for Triangulated 2-Manifolds. In *Visualization and Mathematics III*. Springer, 35–57. https://doi.org/10.1007/978-3-662-05105-4_2

Rahul Mitra, Erick Jimenez Berumen, Megan Hofmann, and Edward Chien. 2024. Singular Foliations for Knit Graph Design. In *ACM SIGGRAPH 2024 Conference Papers*. Article 38. https://doi.org/10.1145/3641519.3657487

Rahul Mitra, Liane Makatura, Emily Whiting, and Edward Chien. 2023. Helix-Free Stripes for Knit Graph Design. In *ACM SIGGRAPH 2023 Conference Proceedings*. Article 75. https://doi.org/10.1145/3588432.3591564

Juan Sebastian Montes Maestre, Yinwei Du, Ronan Hinchet, Stelian Coros, and Bernhard Thomaszewski. 2023. Differentiable Stripe Patterns for Inverse Design of Structured Surfaces. *ACM Transactions on Graphics* 42, 4, Article 102 (2023). https://doi.org/10.1145/3592114

Ashish Myles, Nico Pietroni, and Denis Zorin. 2014. Robust Field-Aligned Global Parametrization. *ACM Transactions on Graphics* 33, 4, Article 135 (2014). https://doi.org/10.1145/2601097.2601154

Nicholas Sharp, Yousuf Soliman, and Keenan Crane. 2019. The Vector Heat Method. *ACM Transactions on Graphics* 38, 3, Article 24 (2019). https://doi.org/10.1145/3243651

Richard W. Sharpe. 1997. *Differential Geometry: Cartan's Generalization of Klein's Erlangen Program*. Springer-Verlag.

Amir Vaxman, Marcel Campen, Olga Diamanti, David Bommes, Klaus Hildebrandt, Mirela Ben-Chen Technion, and Daniele Panozzo. 2017. Directional Field Synthesis, Design, and Processing. In *ACM SIGGRAPH 2017 Courses*. Article 12. https://doi.org/10.1145/3084873.3084921

A Discrete Levi-Civita Connection

In this section, we derive the discrete connection given in Equation 10. Following Braune et al. [2024], we first define a parallel-propagated frame on each vertex neighborhood. We can express any point in the one-ring of vertex i using geodesic polar coordinates $(r, \overline{\varphi})$, which measures radial lengths r along the surface and scales angles by a factor of $\frac{2\pi}{\Phi_i}$, where Φ_i refers to the sum of the tip angles at i. In the polar plane, we define a frame $e_r = \frac{\partial}{\partial r}$, $e_{\overline{\varphi}} = \frac{2\pi}{\Phi_i} \frac{\partial}{\partial \varphi}$ which is orthonormal with respect to the polyhedral metric of the mesh. Then our parallel-propagated frame is given explicitly by

$$\begin{pmatrix} e_0 & e_1 \end{pmatrix} = \begin{pmatrix} e_r & e_{\overline{\varphi}} \end{pmatrix} \begin{pmatrix} \cos \overline{\varphi} & \sin \overline{\varphi} \\ -\sin \overline{\varphi} & \cos \overline{\varphi} \end{pmatrix}. \tag{12}$$

Consider now the frames at two neighboring dual vertices $*imj$ and $*ijk$. The hinge map would unfold triangles imj and ijk in the plane, and simply translate the frame from $*imj$ to $*ijk$. Due to the angle scaling of the polar map, our parallel-propagated frame introduces an extra rotation of $\left(\frac{2\pi}{\Phi_i} - 1\right)\varphi_{*ij}$. Hence, in our frame field, the value of the hinge connection along $*ij$ is precisely (if K_i denotes the discrete (integrated) Gaussian curvature))

$$\eta_{*ij} = \left(1 - \frac{2\pi}{\Phi_i}\right)\varphi_{*ij} = -\frac{K_i}{\Phi_i}\varphi_{*ij}. \tag{13}$$

Now we use the expression for the constant-curvature Levi-Civita connection $\alpha = -\frac{1}{2}\kappa r^2 d\overline{\varphi}$ from Appendix B.2 (where κ denotes the pointwise Gaussian curvature). Since the geodesic polar map scales angles by $\frac{2\pi}{\Phi_i}$, the 1-form $d\overline{\varphi}$ is equal to $\frac{\Phi_i}{2\pi}$ times the ordinary angular 1-form $d\varphi$ in the plane. Moreover, the integral of $\frac{1}{2}r^2 d\varphi$ along a plane curve γ is simply equal to the area of the region formed by connecting the endpoints of γ to the origin. Therefore, the integral of the constant-curvature Levi-Civita connection along a dual edge $*ij$ is equal to $\kappa \frac{\Phi_i}{2\pi}$ times the area of the region in the geodesic polar plane formed by connecting the endpoints of $*ij$ to the origin. Since the polar map has constant Jacobian determinant $\frac{2\pi}{\Phi_i}$, we can compute this area as κ times the area formed on the original mesh by connecting the endpoint of $*ij$ to vertex i—which is precisely the half-diamond area A_{*ij} appearing in Equation 10. Thus, the integral of the constant-curvature Levi-Civita connection along a dual edge $*ij$ in our parallel-propagated frame is simply $-\frac{K_i}{A_i}A_{*ij}$.

Unfortunately, these values do not define a valid connection on our mesh, since they generally define incompatible rotations along the two sides of dual edge $*ij$. Writing down the compatibility conditions explicitly may seem nontrivial, but they can easily be expressed by observing that because the set of valid connections is an affine space, every connection can be written as the hinge map plus a discrete dual 1-form. Explicitly, if $\alpha_{*ij} = \eta_{*ij} + \mathring{\alpha}_{*ij}$, then α_{*ji} must be equal to $\eta_{*ji} - \mathring{\alpha}_{*ij}$. A natural way of reconciling the

desired Levi-Civita integrals along the two sides of dual edge $*ij$ is to minimize the area-weighted error

$$\mathcal{E}(\mathring{\alpha}) = \sum_{ij} \left[\tfrac{1}{2} A_{*ij} \left(\eta_{*ij} + \mathring{\alpha}_{*ij} + \tfrac{K_i}{A_i} A_{*ij} \right)^2 \right. \\ \left. + \tfrac{1}{2} A_{*ji} \left(\eta_{*ji} - \mathring{\alpha}_{*ij} + \tfrac{K_j}{A_j} A_{*ji} \right)^2 \right]. \tag{14}$$

The energy is minimized by setting

$$\mathring{\alpha}_{*ij} = \tfrac{1}{A_{*ij}+A_{*ji}} \left(A_{*ji} \left(\eta_{*ji} + \tfrac{K_j}{A_j} A_{*ji} \right) - A_{*ij} \left(\eta_{*ij} + \tfrac{K_i}{A_i} A_{*ij} \right) \right). \tag{15}$$

Substituting the values of η_{*ij} from Equation 13 completes the proof.

B Analytical Behavior of One-Ring Metrics

B.1 Piecewise-flat metric.

The geodesic polar map is easy to visualize: imagine the one-ring made of paper, and bend that into a cone with its discrete Gaussian curvature κ_i. Projecting the cone along the direction of the axis of the cone, we have the geodesic polar map $(r, \bar{\varphi})$ with the origin at the center vertex. Based on the isometry. The dual frame is precisely

$$\theta = \begin{pmatrix} du + \sin \bar{\varphi} \tfrac{\kappa_i}{2\pi} r d\bar{\varphi} \\ dv - \cos \bar{\varphi} \tfrac{\kappa_i}{2\pi} r d\bar{\varphi} \end{pmatrix} \tag{16}$$

where $(u, v) = r(\cos \bar{\varphi}, \sin \bar{\varphi})$. One may verify that $\alpha^{\mathrm{LC}} = -\kappa_i/(2\pi) d\bar{\varphi}$ precisely satisfies $d\theta + \alpha \mathbb{J} \wedge \theta$.

The discrete connection values are given as integrals along dual edges: $\int_{*i} d\theta = \int_{\partial *i} \tfrac{\kappa_i}{2\pi} (v, -u)^T d\bar{\varphi}$, which is the angle weighted average of the boundary coordinates rotated by $90°$, rescaled by $\tfrac{\kappa_i}{2\pi}$.

If calculated in the true geodesic polar map PPF, the hinge connection actually provides the correct integral of $\tau_{*\vec{ij}} = \int_{\vec{ij}} \alpha^{\mathrm{LC}}$. One can see this by assuming the difference in the angles formed at the vertex in the mesh $\Delta\varphi$ will be the rotation angle for parallel transport in the hinge map, the corresponding rotation in the two frames of the PPF would be $\Delta\bar{\varphi}$, the difference provides $\tau_{*\vec{ij}} = -\kappa_i/(2\pi)\Delta\bar{\varphi}$.

B.2 Constant-curvature metric.

For a metric of constant Gaussian curvature K, the normalized 1-form in the $d\bar{\varphi}$ direction is:

$$e^{\bar{\varphi}} = r \sin(\sqrt{K}r)/\sqrt{K} d\bar{\varphi}, \tag{17}$$

which also works in the case $K < 0$, since sin can be turned into sinh when applied to imaginary numbers. To simplify the derivation, we still use the expansion $\sin(x) = x - x^3/6$. Then

$$d\theta = \tfrac{1}{2} K \begin{pmatrix} v \\ -u \end{pmatrix} du \wedge dv, \tag{18}$$

i.e., the integral will be the barycenter coordinates rescaled by half of the pointwise Gaussian curvature. The analytic expression of the Levi-Civita connection is thus $\alpha^{\mathrm{LC}} = -\tfrac{1}{2} K r^2 d\bar{\varphi}$.

C Analytic Minimal-Torsion Trivial Connections

We obtain closed-form expressions for minimal-torsion trivial connections on the sphere by first deriving closed-form expressions on the plane, and then showing that minimal-torsion connections map to minimal-torsion connections by conformal maps. We can thus apply stereographic projection to obtain minimal-torsion trivial connections on the sphere, at which point we can easily achieve any other torsion by adding a given 1-form to our connection.

The planar case. Suppose we have singularities located at positions $\{\mathbf{s}_i = (s_i^x, s_i^y)\}_i$ with target indices $n_i \in \mathbb{Z}$. In the standard frame e_1, e_2 of $\mathbb{R}^2$, the connection 1-form for the Levi-Civita connection is zero. So we can write any metric connection using a real 1-form $\alpha \in \Omega^1(\mathbb{R}^2)$, and it will capture these singularities if its curvature is

$$d\alpha|_{(x,y)} = -\sum_i 2\pi n_i \delta(x - s_i^x, y - s_i^y), \tag{19}$$

where δ is the Dirac δ function. This equation is solved by

$$\alpha^{\mathrm{opt}} = -\sum_i n_i \, d\varphi|_{(x-s_i^x, y-s_i^y)}, \tag{20}$$

where $d\varphi$ is the angle 1-form

$$d\varphi|_{(x,y)} = \tfrac{1}{x^2+y^2}(-y\, dx + x\, dy). \tag{21}$$

We can always add a gradient to α^{opt} to get another solution, but α^{opt} is the minimum-norm solution, and hence describes the minimal-torsion connection with this curvature.

Finally, we can easily integrate α^{opt} along any line segment by observing that the integral of $d\varphi$ along a line segment measures the angle between the endpoints when viewed from the origin. Using the integral of α^{opt}, we obtain parallel vector fields from our minimal-torsion trivial connection.

Transformation under conformal maps. Let M be a surface with metric g, and fix an orthonormal frame E and with solder form θ. If $\tilde{g} := e^{2u} g$ is a conformally rescaled metric, then the frame $\tilde{E} := e^{-u} E$ is orthonormal with respect to $\tilde{g}$, and the dual frame is $\tilde{\theta} := e^u \theta$.

Now, suppose we have a connection 1-form $\tilde{\omega}$ compatible with metric $\tilde{g}$ written with respect to frame $\tilde{E}$. So $\tilde{\omega}$ has the form $\tilde{\omega} = \mathbb{J}\tilde{\alpha}$.

We can apply a change of frame to $\tilde{\omega}$ to express our connection in frame E. We obtain

$$\tilde{\omega}^{(E)} = \left(e^{-u}\right) \tilde{\omega} \left(e^{-u}\right)^{-1} + \left(e^{-u}\right) d \left(\mathbb{I} e^{-u}\right)^{-1} \tag{22}$$

$$= \tilde{\omega} + \mathbb{I} du \tag{23}$$

$$= \begin{pmatrix} du & -\tilde{\alpha} \\ \tilde{\alpha} & du \end{pmatrix} \tag{24}$$

Intuitively, when seen from E, parallel transport by $\tilde{\omega}$ rotates vectors by $-\alpha$ the same way it did in frame $\tilde{E}$ but now scales them by $-du$ as well. If we ignore the scaling and "project" $\tilde{\omega}^E$ to be compatible with our original metric g, we get a new g-compatible connection

$$\mathrm{Proj}\left(\tilde{\omega}^{(E)}\right) = \mathbb{J}\tilde{\alpha}, \tag{25}$$

which is just our original expression for $\tilde{\omega}$. Note that $\tilde{\omega}^{(E)}$ and $\mathrm{Proj}(\tilde{\omega}^{(E)})$ have the same curvature, since they differ by a du term whose exterior derivative is zero.

Now, we can look at how torsion changes under our change of frame. The torsion of $\tilde{\omega}$ in frame $\tilde{E}$ is given by

$$\tilde{\Theta} := d\tilde{\theta} + \tilde{\omega} \wedge \tilde{\theta}. \tag{26}$$

If we expand out the definitions, we find that

$$\tilde{\Theta} = e^u \left(du \wedge \theta + d\theta + \tilde{\omega} \wedge \theta \right), \tag{27}$$

and therefore,

$$d\theta + \tilde{\omega} \wedge \theta = e^{-u}\tilde{\Theta} - du \wedge \theta. \tag{28}$$

Applying Equation 25 reveals that

$$d\theta + \text{Proj}\left(\widetilde{\omega}^{(E)}\right) \wedge \theta = e^{-u}\widetilde{\Theta} - du \wedge \theta, \tag{29}$$

or equivalently, the torsion of $\text{Proj}(\widetilde{\omega}^{(E)})$ is equal to $e^{-u}\widetilde{\Theta} - du \wedge \theta$. Finally, one can check that $du \wedge \theta$ is exactly equal to $(\star du)^{\sharp} dA$, where the sharp operator and area form come from the original metric g. In summary, if we start with a connection $\widetilde{\omega}$ with torsion $\widetilde{\Theta}$, then applying a conformal transformation and projecting the resulting 1-form to be compatible with the new metric yields a connection with the desired curvature and torsion equal to $e^{-u}\widetilde{\Theta} - (\star du)^{\sharp} dA$.

Since we are interested in the case of the sphere, and we know that $\text{Proj}(\widetilde{\omega}^{(E)})$ has the correct curvature, it suffices to check that the divergence of its torsion is zero whenever the divergence of $\widetilde{\Theta}$ is zero. More formally, let $\widetilde{T}$ be the vector field such that $\widetilde{\Theta} = \widetilde{T} d\widetilde{A}$, and similarly let T be the vector field such that $e^{-u}\widetilde{\Theta} - (\star du)^{\sharp} dA = T dA$.

We wish to show that $\text{div}_{\widetilde{g}}\,\widetilde{T} = 0$ if and only if $\text{div}_g\,T = 0$. Since $d\widetilde{A} = e^{2u} dA$, we have $\widetilde{\Theta} = e^{-u} e^{2u} \widetilde{T} dA$, and therefore $T = e^u \widetilde{T} - (\star du)^{\sharp}$.

$$\text{div}_g\,T = \text{div}_g\left(e^u \widetilde{T} - (\star du)^{\sharp}\right) \tag{30}$$

$$= \text{div}_g\left(e^u \widetilde{T}\right) \tag{31}$$

$$= e^u \,\text{div}_{\widetilde{g}}\left(\widetilde{T}\right), \tag{32}$$

the first step uses the fact that $(\star du)^{\sharp}$ is divergence-free (since it is a rotated gradient), and the second fact uses the transformation rule for the divergence of a vector field under a conformal change of metric. Since e^u is nonzero, we conclude that $\text{div}_g\,T = 0$ if and only if $\text{div}_{\widetilde{g}}\,\widetilde{T} = 0$. So our projected connection has minimal torsion if and only if our original did, as desired.